Superlattices and Microstructures 128 (2019) 151–156

Contents lists available at ScienceDirect

Superlattices and Microstructures

journal homepage: www.elsevier.com/locate/superlattices

Theoretical optimization of inhomogeneous broadening in InGaN/GaN MQWs to polariton splitting at low temperature

Xiaoling Shi, Hao Long*, JinZhao Wu, Lan Chen, Leiying Ying, Zhiwei Zheng, Baoping Zhang**

Department of Electronic Engineering, Optoelectronics Engineering Research Center, School of Electronic Science and Engineering (National Model Microelectronics College), Xiamen University, Xiamen, 361005, China

ARTICLE INFO

Keywords:
Exciton polariton
InGaN/GaN MQWs
Inhomogeneous broadening

ABSTRACT

Exciton-photon interaction in strong coupling region is an interesting topic in exploring bosonic physics and devices. Until now, however, InGaN based exciton polariton was rarely reported since its large inhomogeneous broadening. In this study, the impact of inhomogeneous broadening Γ_{inh} of InGaN/GaN quantum wells (QWs) on the normal mode energy splitting Ω_{NMS}, between the upper and lower polariton branches was theoretically analyzed by transfer matrix method and linear nonlocal dispersion model. Surprisingly, an optimal inhomogeneous broadening Γ_{opt}, corresponding to the maximum value of Ω_{NMS} was deprived at low temperature, which has not been reported before. The effect of Γ_{inh} was divided into two regions for explaining the existence of Γ_{opt}. Meanwhile, the Γ_{opt} was found to be strongly correlated with the oscillator strength and homogeneous broadening.

1. Introduction

Exciton-polariton is a quasi-particle formed by the strong coupling between photon and exciton, which is promising for the high temperature Boson Einstein Condensation (BEC) [1] and zero-threshold polariton lasing [2]. Since C. Weisbuch [3] firstly introduced the planar microcavity into semiconductor polariton region, the research of exciton-polariton has progressed remarkably in fundamental physical research and novel devices [4]. The strong coupling between exciton and photon as well as polariton lasing have been successfully observed in CdTe [5], ZnO [6], GaAs [7], bulk GaN [8], GaN/AlGaN quantum wells (QWs) [9] and perovskite [10] materials etc.

InGaN/GaN QWs exhibited spectacular high quantum efficiency in visible light luminescence, promoting the solid-state lighting technology. Via continually tuning the Indium concentration, InGaN/GaN QWs could cover the full visible spectrums [11]. Therefore, realization of exciton polariton in InGaN/GaN QWs structure is meaningful and will be a firm step toward low-threshold lasing. Until now, however, there are only a few reports on the observation of exciton polariton in InGaN/GaN QWs structure [12,13]. Polariton lasing is still not realized yet, which was ascribed to the detrimental inhomogeneous broadening in InGaN alloys. In last decade, G. Christmann et al. [14] and M. Glauser et al. [15,16] theoretically analyzed the role of inhomogeneous broadening in polaritonic splitting of InGaN/GaN MQWs at room temperature, which predicted tough conditions for realizing strong coupling in RT InGaN/GaN MQWs systems and monotonous decreasing of normal mode splitting with the inhomogeneous broadening. However, the effect

* Corresponding author.
** Corresponding author.
E-mail addresses: longhao@xmu.edu.cn (H. Long), bzhang@xmu.edu.cn (B. Zhang).

https://doi.org/10.1016/j.spmi.2019.01.021
Received 1 November 2018; Received in revised form 17 January 2019; Accepted 22 January 2019
Available online 25 January 2019
0749-6036/

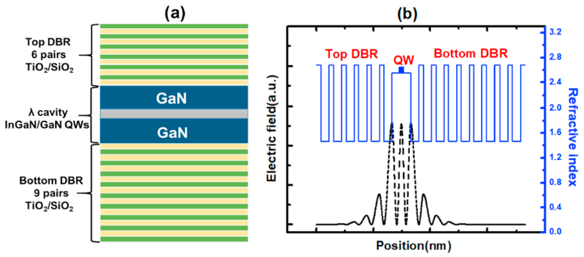

Fig. 1. (a) Schematic diagram of InGaN/GaN QWs microcavity. (b) electric field intensity and refractive index along the vertical direction of microcavity.

of inhomogeneous broadening at low temperature has still be unraveled. In our opinion, to understand the fundamental physics in InGaN based polariton, it is necessary to lucubrate this bosonic system at low temperature.

In this paper, we theoretically studied the relationship between inhomogeneous broadening and normal mode energy splitting in various temperatures by transfer matrix method and linear nonlocal response dispersion model. At room temperature, our results agreed well with earlier literature [14–16], showing monotonous decreasing of polaritonic splitting with inhomogeneous broadening. However, surprisingly at low temperatures, there is an optimal inhomogeneous broadening Γ_{opt} where largest normal splitting between upper and lower polariton branches was anticipated. The dependence of the Γ_{opt} with excitonic oscillator strength and homogeneous broadening was also investigated. We believed that our result could pave a way for refining InGaN polariton research.

2. Theoretical model

In this paper, we investigated the strong coupling between exciton and photon in InGaN/GaN MQWs by transfer matrix methodology and linear nonlocal response dispersion model. In our theoretical model, the microcavity consists of a top and bottom distributed Bragg reflectors (DBR) with 6 and 9 pairs of TiO_2/SiO_2 respectively, and 5 pairs of $In_{0.1}Ga_{0.9}N$/GaN MQWs located at the antinode of optical field of 1λ -thick GaN layer to maximize the light-matter interaction. The luminescence central peak of InGaN/GaN MQWs were set to be 3.0eV, which was a typical color of InGaN blue LED. Fig. 1(a) and (b) show the structure and the stationary electric field intensity in micro-cavity. The width of InGaN wells were set to be from 0.8 nm to 4 nm, while the GaN barrier thickness was fixed to be 6 nm.

The relevant parameters of GaN and InN were cited from Refs. [17–19]. The value of $In_{0.1}Ga_{0.9}N$ were evaluated from the linear interpolation from the values of GaN and InN. The ratio of conduction band offset and valence band offset was set to be ΔE_c**?**$\Delta E_V = 7:3$ [20].

2.1. Oscillator strength

To simulate the absorption spectrum of micro-cavity, oscillator strength of exciton should firstly be determined. The oscillator strength will affect the radiative damping rate and exciton binding energy. Higher oscillator strength would induce stronger coupling strength, larger Rabi splitting as well as larger normal mode splitting. In InGaN/GaN QWs structure, the built-in electric field, thickness of quantum wells (d_w) and some other parameters could be artificially used to manipulate the oscillator strength.

To obtain the oscillator strength of exciton, the built-in electric field strength F, ground energies and wave functions of electrons and holes and the exciton binding energy E_b were firstly calculated. The values of built-in electric field are expressed as:

$$\begin{cases} F_{InGaN} = \left|\dfrac{2(P_{InGaN}-P_{GaN})d_b}{2\varepsilon_{e,InGaN}\varepsilon_0 d_b+\varepsilon_{e,GaN}\varepsilon_0 d_w}\right| \\ F_{GaN} = \left|\dfrac{(P_{GaN}-P_{InGaN})d_w}{2\varepsilon_{e,InGaN}\varepsilon_0 d_b+\varepsilon_{e,GaN}\varepsilon_0 d_w}\right| \end{cases} \tag{1}$$

Where $\varepsilon_{e,InGaN}$ and ε_{GaN} are the dielectric constants of $In_xGa_{1-x}N$ and GaN, d_w and d_b are the widths of quantum wells and barrier layers, respectively [21]. Appling the built-in electric field, Schrodinger equation was utilized for solving the electron and hole in quantum wells [22]. The ground energy and wave functions of electron and hole, and exciton binding energy based on the fractional-dimensional method [23] could be derived. Knowing the built-in electric field, wave function, and binding energy, the exciton oscillator strength can then be calculated. It depends on the quantum transit matrix elements M, the excitonic transition energy E_{ex} and the wave function of electron and hole f_e,f_h,:

$$f = \frac{2M_{QW}M^2}{m_0 E_{ex}}\left|\int_{-\infty}^{+\infty} dz f_e(z) f_h(z)\right|^2 |\varphi(0)|^2 \tag{2}$$

Where M_{QW} is polarization factor, m_0 is the free electron mass [24].

2.2. Transfer matrix

Transfer matrix method has been widely utilized to describe the reflection, transmission and absorption spectrums of stacked multi dielectric layers [25]. In this paper, we adjusted the optical constants of InGaN layers by introducing the linear nonlocal response dispersion model of excitonic oscillators.

The transfer matrix of single quantum well is [26]:

$$M_w = \begin{bmatrix} e^{i\phi_w}(1+i\eta) & i\eta \\ -i\eta & e^{-i\phi_w}(1-i\eta) \end{bmatrix} \tag{3}$$

Where $\phi_w = d_w n/c$; n is the refraction index of quantum well. η can be written as [27]:

$$\eta = \frac{\pi}{n_c}\frac{e^2}{4\pi\varepsilon_0}\frac{f_{osc}}{m_e c}\frac{\tilde{\chi}}{\alpha} \tag{4}$$

$\tilde{\chi}$ is the susceptibility induced by excitonic oscillators. In the presence of Gaussian inhomogeneous broadening $G(w)$, the susceptibility $\tilde{\chi}$ became the convolution of homogeneous Lorentzian function and inhomogeneous Gaussian distribution [28]:

$$\tilde{\chi}(w) = \int \frac{(\varepsilon_B w_{LT} a_B^3 w_0^2/4c^2)}{w_0-(w-\nu)-i\Gamma_h} G(\nu - w_0)d\nu = i\frac{(\varepsilon_B w_{LT} a_B^3 w_0^2/4c^2)\sqrt{\pi}}{\Gamma_{inh}} e^{-z^2} erfc(-iz) \tag{5}$$

Where $z = \frac{w-w_0+i\Gamma_h}{\Gamma_{inh}}$, w_{LT} and a_B^3 are the longitudinal-transverse splitting and Bohr radius of exciton in the bulk material; erfc(z) is the complementary error function; Γ_h is the non-radiative homogeneous broadening; Γ_{inh} is the inhomogeneous broadening.

The total transfer matrix across a structure containing m layers has the form [29]:

$$M = \prod_{j=1}^{2m+1} M_j \tag{6}$$

The amplitude reflection and transmission coefficients satisfied:

$$\begin{bmatrix} t \\ 0 \end{bmatrix} = \begin{bmatrix} M_{11} & M_{12} \\ M_{21} & M_{22} \end{bmatrix}\begin{bmatrix} 1 \\ r \end{bmatrix} \tag{7}$$

where r and t represented reflection and transmission coefficients of amplitude of the electric field.

3. Results and discussion

Based on the above transfer matrix method, the absorption spectrum A(w) was calculated by: A(w) = 1-T(w)-R(w); where T(w) and R(w) represented transmission and reflection spectrums respectively. The absorption comes from the imaginary of complex dielectric constants originated from exciton oscillator resonance. Fig. 2 shows a typical absorption spectrum by our method under the condition of 11 meV inhomogeneous broadening, 5 K temperature and 2nm/6 nm InGaN/GaN QWs. Two peaks originated from the low and upper branches of exciton polariton by strong coupling. The normal mode splitting was about 33.9 meV.

The normal mode splitting Ω_{NMS} hereby was defined by the splitting between upper branch (UP) and lower polariton branch (LP) at the normal incidence geometry, and can be expressed as $\Omega_{NMS} = \sqrt{\Omega_{Rabi}^2 + \delta^2}$, where Ω_{Rabi} is the Rabi splitting, δ is the detuning value. In this simulation, we artificially equalized the center of exciton luminescence (3.0eV) and the cavity mode (nominal zero detuning). It should be noticed that the profound inhomogeneous broadening in InGaN will generate certain exciton diverging from zero detuning condition. In later discussion, it will be seen that this renders special dependence of the normal splitting Ω_{NMS} on the

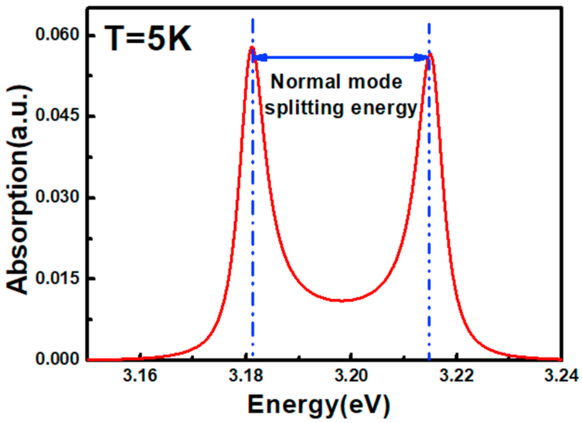

Fig. 2. Simulated normal incidence absorption spectrum at T = 5 K

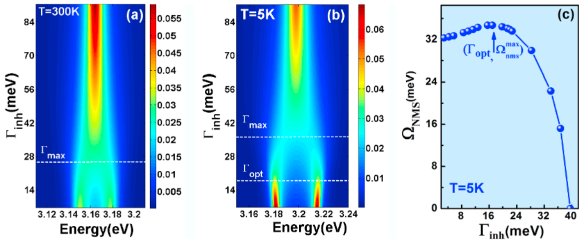

Fig. 3. Simulated normal incidence absorption spectrum as the function of inhomogeneous broadening at (a) T = 300 K, (b) T = 5 K; and (c) normal mode splitting dependence on the inhomogeneous broadening at 5 K.

Γ_{inh} at low temperatures.

To have a clear recognition about the relationship between the normal mode splitting Ω_{NMS} and the inhomogeneous broadening Γ_{inh}, we display in Fig. 3(a) and (b) the absorption spectrum mapping with different Γ_{inh} at T = 300 K and T = 5 K with d_w = 2 nm. Two critical inhomogeneous broadening values could be derived from the illustrations: Γ_{opt} and Γ_{max}. There is a maximum inhomogeneous broadening Γ_{max}, above which the normal splitting cannot be distinguished. The value of Γ_{max} at T = 5 K was 38 meV, higher than the value of 27 meV at T = 300 K. Our results agreed well with former reports by G. Christmann et al. [14] and M. Glauser et al. [15,16], which published similar data at room temperature. More interestingly, in Fig. 3(b) and (c), Ω_{NMS} at T = 5 K increased as Γ_{inh} increasing until an optimal inhomogeneous broadening Γ_{opt}, while no such phenomena were observed in 300 K (Fig. 3(a)). Since previous papers focused on room temperature, no such data has been reported before.

Photons in micro-cavity can only couple with excitons within certain energy range around the center. Under small detuning, although almost all excitons can strongly couple with cavity photon, but the absolute effective detuning $|\delta_{eff}| = \int_{w_-}^{w_+} |\delta(w)|\cdot I(w)dw$ was not zero (where I(w) is the exciton spectrum, $w_{+(-)}$ is the up (low) limit of exciton, $|\delta(w)| = |E(c) - \hbar w|$). Referring to the equation: $\Omega_{NMS} = \sqrt{\Omega_{Rabi}^2 + |\delta_{eff}|^2}$, the normal splitting energy will increase by absolute effective detuning $|\delta_{eff}|$. By increasing Γ_{inh}, average effective detuning between exciton and photon will increase. This could be explained by Fig. 4(a).

Two regions were defined by inhomogeneous broadening: region I with small inhomogeneous broadening, constant Rabi splitting and increasing $|\delta_{eff}|$; region II with larger inhomogeneous broadening, decreasing Rabi splitting and quenching normal mode splitting. Γ_{opt} occurs at the border between these two regions.

In region I, Ω_{NMS} would increase by the inhomogeneous. For specification, an extremely simplified situation with perfect cavity mode (denoted by 'C') and exciton modes ('X') with zero homogeneous broadening were assumed in Fig. 4(b) and (c). In Fig. 4(b), corresponding to the zero inhomogeneous broadening, the UP and LP splits with Ω_{Rabi} energy interval. In Fig. 5(c), single exciton in Fig. 4(b) was separated into two excitons (X+ and X-) by 2Δ inhomogeneous broadening. Both exciton 'X+' and 'X-' will couple with cavity photon ('C') separately with normal mode splitting of $\sqrt{\Omega_{Rabi}^2 + \Delta^2}$, leading two UP ($UP_+$, UP−) and two LP ($LP_+$, LP-) branches. Therefore, the normal mode splitting between average UP = (UP− + UP_+)/2 and LP = (LP- + LP_+)/2 was $\sqrt{\Omega_{Rabi}^2 + \Delta^2}$, which was larger than the counterpart of zero inhomogeneous case in Fig. 4(b).

However, further increasing Γ_{inh} into region II, some portion of exciton will lose strong coupling with photons, the coupling strength and Rabi splitting will reduce by $\Omega_{Rabi} \propto \sqrt{N_{exc}}$ (N_{exc} denotes the coupled exciton density), leading to the decline of normal mode splitting [7].

To further explore the intrinsic mechanism, the temperature and well width were varied to uncover the dependence of Γ_{opt}. We firstly analyzed the Γ_{opt} as function of the quantum well width d_w. Fig. 5(a) illustrated the dependence of Ω_{NMS} on Γ_{inh} and d_w at 5 K. Under the same Γ_{inh}, the Ω_{NMS} would decrease as widening of quantum wells. This could be understood by the decrease of exciton oscillator strength f_{osc} and separation of holes and electrons in the wells, resulting in the reduction of Rabi splitting Ω_{Rabi}. Meanwhile, at any well width, the Ω_{NMS} increased firstly and then decrease by Γ_{inh} at T = 5 k with an optimal inhomogeneous broadening value Γ_{opt}. The value of Γ_{opt} was sensitive to the well width. Fig. 5(b) reveals the dependence of the optimal inhomogeneous broadening Γ_{opt} on the well width at 5 K. It shows that Γ_{opt} decreased by quantum well thickness. Meanwhile, the relationship between f_{osc} and Γ_{opt} was given in Fig. 5(c). The Γ_{opt} were almost proportional to f_{osc}. The oscillator strength was representation of the exciton binding energy

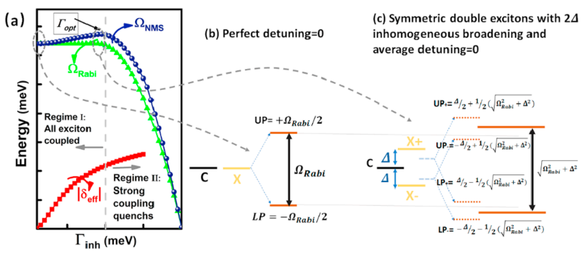

Fig. 4. (a) Two regions defined by inhomogeneous broadening in determine normal mode splitting; energy schemes of (b) perfect zero detuning; and (c) simplified double excitons with average zero detuning, 2Δ inhomogeneous broadening and larger mode splitting.

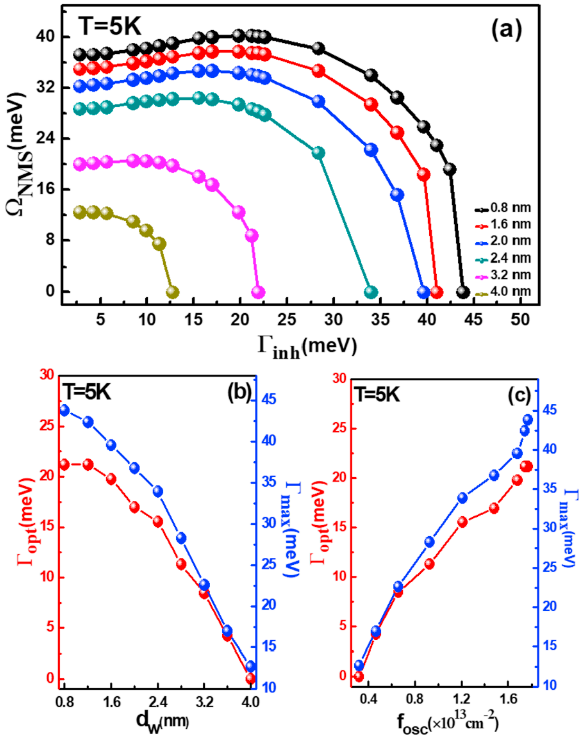

Fig. 5. (a) Simulated Ω_{NMS} as a function of Γ_{inh} with different well width dw = 0.8 nm, 1.6 nm, 2.0 nm, 2.4 nm, 3.2 nm, 4 nm at T = 5 K. (b) Γ_{opt} and Γ_{max} as function of well width at T = 5 K. (c) Γ_{opt} and Γ_{max} as a function of f_{osc}.

per volume and was one of the pivotal factors influencing Rabi splitting value. Therefore, higher oscillator strength induced stronger coupling and more robustness of exciton polariton. Thus, we can enhance the Γ_{opt} by elevating the value of f_{osc}, such as: optimizing the thickness of barriers' and wells' thickness, increasing the overlap between hole and electrons etc. By the way, the dependence of

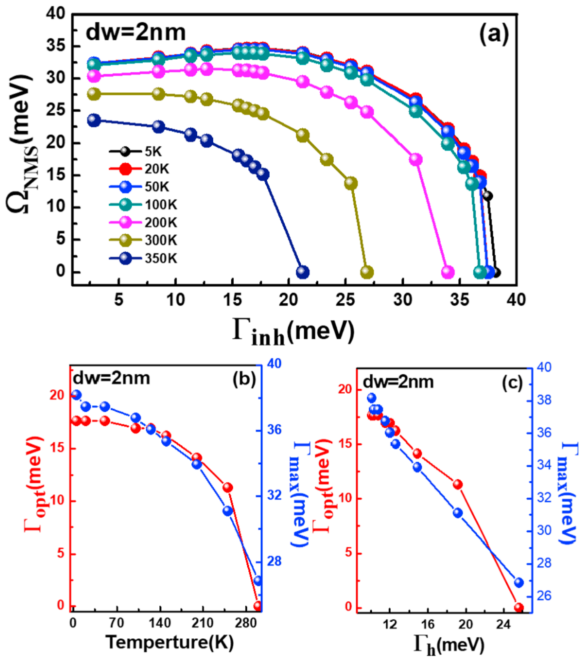

Fig. 6. (a) Simulated Ω_{NMS} as a function of Γ_{inh} for the well width dw = 2 nm at the temperature T = 5 K,20 K,50 K,100 K,200 K,300 K, 350 K. (b) Γ_{opt} and Γ_{max} as a function of temperature. (c) Γ_{opt} and Γ_{max} as a function of Γ_h.

maximum tolerable inhomogeneous broadening Γ_{max} with f_{osc} was also deprived and concerted with previous reports [14–16].

Besides the quantum well thickness, temperature also influences the normal mode splitting Ω_{NMS}. Fig. 6(a) shows that, at lower temperatures (< 200 K), keeping $d_w = 2$ nm, Ω_{NMS} increased by Γ_{inh} until Γ_{opt} and then decreased. However, at high temperatures (T > 200 k), the Ω_{NMS} decreases monotonously by Γ_{inh}. In Fig. 6(b), Γ_{opt} decreased by temperature with $\Gamma_{opt} = 0$ meV at room temperature, which explained why no such experiments reported at T = 300 K. From the relationship between temperature and homogeneous broadening [30]: $\Gamma_h = \gamma_{ph}T + \frac{\Gamma_{LO}}{\exp(E_{LO}/K_BT) - 1}$, (where γ_{ph} means the interaction between exciton and acoustic phonon, and Γ_{LO} is the exciton-LO phonon broadening), we displayed in Fig. 6(c) the Γ_{opt} as function of Γ_h. It was clear that Γ_{opt} was inversely proportional to Γ_h. The convolution of Γ_h and Γ_{inh} determines the final Ω_{NMS}. Reduction of Γ_h would increase the Γ_{opt}.

4. Conclusion

In conclusion, the normal mode splitting Ω_{NMS}, between lower and upper branches of exciton-polaritons in InGaN/GaN MQWs based micro-cavity was theoretically studied. Beside the maximum inhomogeneous broadening Γ_{max}, an optimal inhomogeneous broadening Γ_{opt}, corresponding to the maximum value of Ω_{NMS} at low temperature was also predicted. Two regions were defined to describe the effect of inhomogeneous broadening. The existence of Γ_{opt} was explained by the increasing of absolute effective detuning. Γ_{opt} was further found to be related with exciton oscillator strength and homogeneous broadening. Our calculation will be helpful for experimentally realizing InGaN polaritons.

Acknowledgement

This work was supported by the National Key Research and Development Program of China (No. 2016YFB0400803), the National Natural Science Foundation of China (Nos. 61704140, 11474235, U1505253), the President Funding of XMU (20720180098) and the Science Challenge Project (No. TZ2016003).

References

[1] J. Kasprzak, M. Richard, S. Kundermann, Nature 443 (2006) 409.
[2] A. Kavokin, G. Malpuech, F.P. Laussy, Phys. Lett. A 306 (2003) 187.
[3] C. Weisbuch, M. Nishioka, A. Ishikawa, Y. Arakawa, Phys. Rev. Lett. 69 (1992) 3314.
[4] T.C.H. Liew, A.V. Kavokin, I.A. Shelykh, Phys. Rev. Lett. 101 (2008) 016402.
[5] R. Huang, Y. Yamamoto, R. Andre´, J. Bleuse, M. Muller, et al., Phys. Rev. B 65 (2002) 165314.
[6] R. Shimada, J. Xie, V. Avrutin, et al., Appl. Phys. Lett. 92 (2008) 011127.
[7] H. Deng, G. Weihs, D. Snoke, et al., Proc. Natl. Acad. Sci. Unit. States Am. 100 (2003) 15318.
[8] S. Christopoulos, G.B. von Högersthal, A.J. Grundy, Phys. Rev. Lett. 98 (2007) 126405.
[9] G. Christmann, R. Butte´, E. Feltin, J. Carlin, N. Grandjean, Appl. Phys. Lett. 93 (2008) 051102.
[10] R. Su, C. Diederichs, J. Wang, et al., Nano Lett. 17 (2017) 3982.
[11] S. Nakamura, T. Mukai, M. Senoh, et al., Appl. Phys. Lett. 64 (1994) 1687.
[12] T. Tawara, H. Gotoh, T. Akasaka, et al., Phys. Stat. Sol. 2 (2005) 809.
[13] T.C. Lu, J.R. Chen, S.C. Lin, S.W. Huang, S.C. Wang, Y. Yamamoto, Nano Lett. 11 (2011) 2791–2795.
[14] G. Christmann, R. Butte, E. Feltin, J.F. Carlin, N. Grandjean, Phys. Rev. B 73 (2006) 153305.
[15] M. Glauser, G. Rossbach, G. Cosendey, J. Levrat, M. Cobet, J.F. Carlin, J. Besbas, M. Gallart, P. Gilliot, R. Butte, N. Grandjean, Phys. Status Solidi C (2012) 1–5.
[16] M. Glauser, C. Mounir, G. Bossbach, E. Feltin, J.F. Carlin, R. Butte, N. Grandjean, J. Appl. Phys. 115 (2014) 233511.
[17] T. Takeuchi, H. Amano, I. Akasaki, Jpn. J. Appl. Phys. 1 (39) (2000) 413.
[18] A. Asgari, K. Khalili, Sol. Energy Mater. Sol. Cells 95 (2011) 3124.
[19] I. Vurgaftman, J.R. Meyer, L.R. Ram-Mohan, J. Appl. Phys. 89 (2001) 5815.
[20] G. Martin, A. Botchkarev, A. Rockett, et al., Appl. Phys. Lett. 68 (1996) 2541.
[21] Shi Jun-jie, Gan Zi-zhao, J. Appl. Phys. 94 (2003) 407.
[22] D.C. Hutchings, Appl. Phys. Lett. 55 (1989) 1082.
[23] H. Mathieu, P. Lefebvre, P. Christol, Phys. Rev. B 46 (1992) 4092.
[24] B. Zhang, S.S. Kano, Y. Shiraki, R. Ito, Phys. Rev. B 50 (1994) 7499.
[25] V. Savona, Linear Optical Properties of Semiconductor Microcavities with Embedded Quantum Wells, Springer Berlin Heidelberg, 1999.
[26] L.I. Deych, M.V. Erementchouk, A.A. Lisyansky, Phys. Rev. B 69 (2004) 075308.
[27] M.S. Skolnick, T.A. Fisher, D.M. Whittaker, Semicond. Sci. Technol. 13 (1998) 645.
[28] L.C. Andreani, G. Panzarini, A.V. Kavokin, M.R. Vladimirova, Phys. Rev. B 57 (1998) 4670.
[29] E.L. Ivchenko, Sov. Phys. Solid State 33 (1991) 1344.
[30] A.J. Fischer, W. Shan, J.J. Song, et al., Appl. Phys. Lett. 71 (1997) 1981.